Materials Today Communications

Study on the cytocompatibility, mechanical and antimicrobial properties of 3D printed composite scaffolds based on PVA/ Gold nanoparticles (AuNP)/ Ampicillin (AMP) for bone tissue engineering

--Manuscript Draft--

Manuscript Number:	MTCOMM-D-21-00231R1
Article Type:	Full Length Article
Section/Category:	Biomaterials and biomedicine
Keywords:	Gold nanoparticle; PVA; Ampicillin; 3D Printing; Bone tissue engineering
Corresponding Author:	Deepak M Kalaskar, PhD UCL: University College London London, UNITED KINGDOM
First Author:	Aysenur TOPSAKAL
Order of Authors:	Aysenur TOPSAKAL
	Swati Midha, PhD
	Esra Yuca
	Hilal Turkoğlu Sasmazel, PhD
	Arı Tukay, MSc
	Deepak M Kalaskar, PhD
	Oguzhan Gunduz, PhD
Abstract:	Over the years, gold nanoparticles (AuNP) have been widely used in several biomedical applications related to the diagnosis, drug delivery, bio-imaging, photo-thermal therapy and regenerative medicine, owing to their unique features such as surface plasmon resonance, fluorescence and easy surface functionality. Recent studies showed that gold nanoparticles display positive effect on osteogenic differentiation. In line with this effect, 3-Dimesional (3D) scaffolds that can be used in bone tissue were produced by exploiting the properties of gold nanoparticles that increase biocompatibility and support bone tissue development. In addition, ampicillin was added to the scaffolds containing gold nanoparticles as a model drug to improve its antimicrobial properties. The scaffolds were produced as composites of polyvinyl alcohol (PVA) main matrix as PVA, PVA/AuNP, PVA/Ampicillin (AMP) and PVA/AuNP/AMP. Scanning Electron Microscopy (SEM) Fourier Transform Infrared Spectroscopy (FTIR), tensile measurement tests, and in vitro applications of 3D scaffolds were performed. As depicted by SEM, scaffolds were produced at pore sizes appropriate for bone tissue regeneration. According to FTIR results, there was no modification observed in the AMP, PVA and gold nanoparticles due to mixing in the resultant scaffolds. In vitro results show that 3D printed composite scaffold based on PVA/AuNP/AMP are biocompatible, osteo-inductive and exhibit antimicrobial properties, compared to PVA scaffolds. This study has implications for addressing infections during orthopedic surgeries. The PVA-based gold nanoparticle 3D tissue scaffold study containing ampicillin covers a new study compared to other articles based on gold nanoparticles.
Suggested Reviewers:	Apurba Das, PhD Professor, Indian Institute of Technology Indore apurba.das@iiti.ac.in expert in manufacturing of biomaterials and their characterization, 3D printing
	Alan M Smith, PhD Professor, University of Huddersfield a.m.smith@hud.ac.uk expert in biopolymers, 3D printing and materials characterization
	S Dhakshinamoorthy, PhD

	Assistant Professor, SASTRA Deemed University: Shanmugha Arts Science Technology and Research Academy dhakshinamoorthy@scbt.sastra.edu expert in bone engineering and biomaterials
Opposed Reviewers:	
Response to Reviewers:	

Reviewer 1

1. Please highlight the innovation.

- The PVA-based gold nanoparticle 3D tissue scaffold study containing ampicillin covers a new study compared to other articles based on gold nanoparticles. **The innovation has been highlighted in the introduction section as follows:**

"As discussed above, the complexity of the bone structure and the high destruction caused by bone injuries often leads to complications in bone healing. Here, the application of bespoke bone substitutes will be useful in terms of providing a patient-specific and defect-specific support to restore the original properties of the injured bone tissue. In addition, to combat post-surgical infections, which are either implant-associated contaminations, hospital-led or systemic bacterial invasion from other sites, the innovative concept of surgical implantation of osteogenic-inducing scaffolds with appropriate porosity combined with an antibacterial activity, can provide a more efficient strategy for the regeneration of elective bone defects [1]. Thus the novelty of our work lies in the fabrication of PVA-based 3D printed composites, reinforced with AuNPs and AMP, to develop multi-functional biomaterials for orthopedic applications, with the following objectives: (1) 3D printed PVA-based scaffolds for the production of bespoke surgical implants for orthopedic applications, (2) Incorporation of AuNPs to promote bone cell proliferation and differentiation, mechanical strength, electrophysiological signaling, and antioxidant activity similar to physiological bone tissue, and (3) Addition of AMP to administer anti-bacterial properties to the implants to combat post-implantation infections.**"**

2. In the "Materials and Methods" section, it was mentioned that the PLA was adopted in this work, but the information of it did not mentioned afterward.

- We thank the reviewer for pointing out this correction, PLA was changed to PVA in 'Materials and Methods' section.

3. All experiments just provided the results and did not discussed in depth.

- Results have been discussed and added into the manuscript.

4. Please explain why the FT-IR peak of AMP at 1764 cm-1 shifted to a lower wavenumber after incorporating into the PVA matrix.

- After incorporating into the PVA matrix, because of the absence of the signal in the region of 1764 cm^{-1} in PVA spectrum, there is a flattening of the peaks in this region.

5. Some state-of-art works concerning simultaneously promoting cell differentiation and antibacterial effects of bone scaffolds may provide some inspiring information to readers, which have to be included.

We have now inlcuded folloiwng recent stuides with similar foscus.

a. A strawberry-like Ag-decorated barium titanate enhances piezoelectric and antibacterial activities of polymer scaffold. Nano Energy, 2020, 74: 104825.

b. Microstructure evolution and texture tailoring of reduced graphene oxide reinforced Zn scaffold." Bioactive Materials 6.5 (2020): 1230-1241.

6. Please explain why the antibacterial effects of PVA/AMP was weaken after introducing AuNP.

- For the antibacterial efficacy of ampicillin, one of the β-lactam antibiotics, the β-lactam ring must remain accessible.Thus, by binding to bacterial transpeptidases, they prevent the covalent cross-linking of peptidoglycans necessary for cell wall construction and growth of bacteria. AuNP-Ampicillin hybrid systems have been the subject of many studies to date and the antibacterial properties of AuNP-Ampicillin conjugates for gram positive and gram negative bacteria have been characterized. In AuNP-Ampicillin hybrids where this type of surface is functionalized, the lactam ring orientation can be adjusted to maintain antibacterial efficacy

(Tarrat, 2014). In our scaffold system, antibiotics and nanoparticles were added as separate components during scaffold fabrication without being subjected to a conjugation process. As a result of the uncontrolled interactions of free gold nanoparticles and ampicillin molecules in the environment, the orientation of the beta-lactam ring may limit binding with bacterial transpeptidases.

In this study, although a decrease in antibacterial effect was observed with the addition of free AuNP to the scaffold system, we reached our goal of keeping the antibacterial activity effective in the 3D printed scaffold system even after processes such as UV application or the addition of gold nanoparticles in the production process.

Tarrat,N., Benoit,M., Giraud, M., Ponchet, A. And Casanove, M. J. , The gold/ampicillin interface at the atomic scale, Nanoscale, 2015. : DOI: 10.1039/c5nr03318g

7. The title was not good enough to reflect the core of your work. It was recommended to revise it.

- The title is changed as 'Study on the cytocompatibility, mechanical and antimicrobial properties of 3D printed composite scaffolds based on PVA/ Gold nanoparticles (AuNP)/ Ampicillin (AMP) for bone tissue engineering'.

Reviewer 2

The manuscript "Antibacterial 3D printed biocomposites of PVA/ Gold nanoparticles for orthopedic applications " is very interesting and is well written. The abstract gives a concise summary of the manuscript. The results are adequate and well analysed. The conclusions highlighted and summarised the contents of the manuscript. More relevant references should be introduced for example: please see below, therefore, minor corrections should be addressed before being accepted.

Following relevent publications are now cited in in this manuscript

1.K. Sehnal et al. In Proceedings of the 2019 Institute of Electrical and Electronics Engineers

(IEEE) International sensors and nanotechnology conference (SENSORS AND NANO 2019), 24-25July 2019, Penang, Malysia. Biophysical analysis of silver nanoparticles prepared by green synthesis and their 4s efor 3D printing of antibacterial material for health care.

Reviewer 3

Overall opinion: The hypothesis and the novelty of this work should be properly stated. The authors suggest the use of ampicillin as the loaded antibiotic into the 3D structure intended to treat for S. aureus bone infection. Considering that for S. aureus, specially MRSA, bone infection the antibiotics are suggested in clinics are not ampicillin (e.g. Vancomycin, Minocycline) what is the rational for the use of an antibiotic that is not suggested for this type of infection? The article is written in acceptable English. In my opinion there are still several aspects to be improved in this paper as discussed below.

- In this study, we designed an antibacterial scaffold system that provides increased osteogenic differentiation as a proof of concept. Considering the pros and cons in terms of antibacterial effect and osteogenic differentiation. In a multifunctional 3-printed scaffold system, we used Ampicillin as the model antibacterial agent and showed its effect on *S. aureus*, which causes osteomyelitis. Likewise, effective antibiotics such as vancomycin and minocycline can also be used against bone infections.

Specific points:

Abstract

1. The authors say "Gold nanoparticles (AuNP) are widely used in diagnosis, drug delivery, biomedical imaging and photo-thermal therapy..". The authors should improve this sentence for clarity. Are nanoparticles (AuNP) widely used in diagnosis, drug delivery, biomedical imaging and photo-thermal therapy in clinics or being proposed to be used in?

- The sentence has been revised for clarity – " Over the years, gold nanoparticles (AuNP) have been widely used in several biomedical applications related to the diagnosis, drug delivery, bioimaging, photo-thermal and regenerative medicine, owing to their unique features such as surface plasmon resonance, fluorescence and easy surface functionality."

2. The abstract content should reflect more on obtained results and conclusion.

- The abstract has been revised with more detailed on results and conclusion.

Introduction section

3. Considering that in S. Aureus, specially MRSA, bone infection the antibiotics are suggested in clinics are not ampicillin (e.g. Vancomycin, Minocycline) what is the rational of an antibiotic that is not suggested this type of infection? (ref. The Sanford Guide to Antimicrobial Therapy). The authors should justify their choice.

- We thank reviewer for pointing this out. We have incorporated this explanation at the end of manuscript:

In this study, we designed an antibacterial scaffold system and provided proof of concept of increased osteogenic differentiation of the scaffold which could potentially be used as a surgical implant in orthopedic implantations. Considering the limitations of conjugating antibiotics on the resultant osteogenic differentiation of scaffolds, we used antibiotics and gold nanoparticles in free form in this system without creating a hybrid structure. In this multifunctional 3D-printed scaffold system, we used Ampicillin as the model antibacterial agent and showed its effect on *S. aureus*, the primary causative agent for osteomyelitis. The system is simple, robust and economical, hence a broad spectrum of other antibiotics such as vancomycin and minocycline could be easily applied to our system to be used against orthopedic infections.

4. Please state clearly the hypothesis of this work and its novelty.

The complexity of the bone structure and the magnitude of the damage are among the difficulties encountered in bone healing. With the use of multi-combination and multifunctional biomaterials, the extracellular matrix is mimicked to further communicate with the biological microenvironment to control and improve osteogenesis and mineralization and even the ability to form blood vessels. AuNPs are exepct to promote cell proliferation, osteogenic while proving mechanical strength, electrophysiological signaling, and antioxidant activity. Simultaneous release of AMP from scaffolds will ensure localized provision of antibacterial properties to prevent infections at the implantation site.

The following paragraph has been added in the end of the introduction –

"As discussed above, the complexity of the bone structure and the high destruction caused by bone injuries often leads to complications in bone healing. Here, the application of bespoke bone substitutes will be useful in terms of providing a patient-specific and defect-specific support to restore the original properties of the injured bone tissue. In addition, to combat post-surgical infections, which are either implant-associated contaminations, hospital-led or systemic bacterial invasion from other sites, the innovative concept of surgical implantation of osteogenic-inducing scaffolds with appropriate porosity combined with an antibacterial activity, can provide a more efficient strategy for the regeneration of elective bone defects [1]. Thus the novelty of our work lies in the fabrication of PVA-based 3D printed composites, reinforced with AuNPs and AMP, to develop multi-functional biomaterials for orthopedic applications, with the following objectives: (1) 3D printed PVA-based scaffolds for the production of bespoke surgical implants for orthopedic applications, (2) Incorporation of AuNPs to promote bone cell proliferation and differentiation, mechanical strength,

electrophysiological signaling, and antioxidant activity similar to physiological bone tissue, and (3) Addition of AMP to administer anti-bacterial properties to the implants to combat post-implantation infections.**”**

5. More recent references on 3D scaffolds for bone treatment should be cited such as:

- Recent references were added into the manuscript.

1. 3D-printed platform multi-loaded with bioactive, magnetic nanoparticles and an antibiotic for re-growing bone tissue. International Journal of Pharmaceutics

Volume 593, 25 January 2021, 120097

2. Engineering a multifunctional 3D-printed PLA-collagen-minocycline-nanoHydroxyapatite scaffold with combined antimicrobial and osteogenic effects for bone regeneration. Materials Science and Engineering: C Volume 101, August 2019, Pages 15-26

Materials section: should be improved.

We have proivided more information for this section on page 5.

6. Provide information on printing conditions specifications (i.e. printing speed, solution viscosity, layer height) and extruder detailed specifications. Slicing software used information should be provided as well as 3D modeling software.

- Before the writing process, a rectangular prism of 20x20x3mm was drawn using the SolidWorks design program. In line with the features expected from the tissue scaffold, besides design controls such as occupancy rate, number of layers, shape and angle; With the Simplify program, which enables the control of process parameters such as speed, temperature and flow rate, a tissue scaffold with a height of 10 times (0.35mm) at +45, -45 angles and 85% fullness was prepared, and pre-printing controls were made on the simulation screen of the program. Subsequently, the design was transformed into a G-Code that the bioprinter could perceive, and made ready for writing.

7. Provide information regarding posprinting finishing.

- Final produced scaffold has 20x20mm dimensions and were approximately 0.35 mm in height. This information has now been added to the results section 3.1.

8. In the sentence "The mechanical properties of the resultant scaffolds were computed by measuring tensile strength". Please replace "computed" by obtained.

- "computed" was replaced by obtained.

9. In the sentence …."PVA/AuNP/AMP) were analyzed by Scanning Electron Microscope (SEM)" Please replace "Microscope " by Microscopy.

- 'Microscope' has been changed to 'Microscopy'

10. page 6. Section "In Vitro Cell Culture". Section name should be improved. Materials/reagents (name with cc, purity, brand/supplier, provenience) used should be removed from the beginning of this section and included when appearing in method description. This will avoid repeating information and ease this section methods. page 7.

- Section " In Vitro Cell Culture" is changed with "Cell Culture Studies". Materials/reagents (name with cc, purity, brand/supplier, provenience) is removed from the beginning of "Cell Culture Studies" section and added in materials and methods section.

11. Scaffolds were placed for 45 min under UV light. What happens to the antibiotic? Could the authors provide a guarantee that some activity of the antibiotic was not lost by the UV-light?

- Elmolla et al has reported the effects of UV on different antibiotics. It has been reported that Ampicillin undergoes a 3.8 % degradation after 3 hours of UV application. Therefore, we hypothesized that 45 minutes of UV application to the surface would cause a very limited amount of degradation of antibiotic in scaffolds. Another detailed study performed by Naveed et al., further, confirmed that UV exposure of 30 mins has minör effect on the degradation of ampicillin and the antibiotic remains within the official limits i.e. 95-105% of the drug should be available in % assay [2]. Based on these previous literature, we decided to apply UV for 45 minutes duration to scaffold surface, as it would possibility cause very limited amount of degradation of the antibiotic in the scaffolds.

Elmolla, E., Chaudhuri M., Degradation of amoxicillin, ampicillin and cloxacillin antibiotics in aqueous solution by the UV/ZnO photocatalytic process, Journal of Hazardous Materials 173 (2010) 445–449.

12. Information on TCPS used as control should be provided. Name, brand/supplier, provenience…

page 8. In the sentence "…pH of the solution was strictly adapted to 4.1-4.3 using HCl...". Please replace "adapted" by adjusted.

- Exponentially growing cells were plated in flat-bottomed 96-well plates (Corning, U.S.A.). MC3T3-E1 mouse osteoblast cells were obtained from the Department of Bioengineering, Kirikkale University (Kirikkale, Turkey).

In page 8, “adapted” is replaced with “adjusted”.

page 9. Regarding the Antimicrobial Activity Assay:

13. More details on the S. aureus used should be provided (i.e. ATTC code, MRSA?,

MSSA?); inoculum concentration should be provided; incubation conditions should be provided; inhibition zone measuring equipment information should be provided.
A control should be used in this assay. A diffusion disk with the antibiotic used under the assay in a concentration described in antimicrobial testing guidelines should be used to assure test suitability and comparation with other experiments.

- S. aureus (ATCC 25923) was used for antibacterial analysis. . The bacterial culture was cultivated in Luria-Bertani (LB) broth (10 g/L bacto-tryptone, 5 g/L yeast extract, 5 g/L NaCl) overnight at 37 oC. 10^7 colony-forming units (CFU/mL) were inoculated on LB-agar plate. The scaffolds were gently placed on the bacteria inoculated agar plates and incubated at 37 °C for 24h. Zones of inhibition of the patches were evaluated by measuring the clear area using a ruler.

The quadruple antimicrobial set used contains a scaffold without antibiotics or nanoparticles as negative control. Here, we used scaffold containing only the antibiotic as a positive control. We thought that using another disc material as a positive control would not provide a complete comparison, as the release of the antibiotic from the polymer in the medium, the thickness of the material, and the surface / weight values will be different. The analysis we will carry out with antibiotic impregnation on the same scaffold material will not provide an accurate comparison for these reasons. We agree with the referee to demonstrate the effectiveness of the antibiotic, we used the antibiotic-only scaffold system as a positive control to perform this correctly.

Results and Discussion: should be improved.

14. page 10. Could the authors please discuss why when joining the antibiotic with AuNps (PVA/ %1 v/v AuNP / %10 w/v AMP) the stress and strain % decreased when comparing to PVA/ %10 w/v AMP or PVA/ %1 v/v AuNP?

- Merchan et al. has reported the effect of increasing antibiotics on the mechanical properties. However, the presence of AMP influences tensile strain and tensile strength significantly. In case of AMP, the effect of its presence in the systems on Young's modulus is hardly noticeable in the investigated range of the antibiotic (up to 1 wt.%). The authors showed that the former mentioned tensile characteristic is reduced at 1 wt.% presence of AMP.

M. Merchan, J. Sedlarikova, M. Friedrich, V. Sedlarik, P. Saha, Thermoplastic modification of medical grade polyvinyl chloride with various antibiotics: Effect of antibiotic chemical structure on mechanical, antibacterial properties, and release activity, Polym. Bull. 67 (2011) 997–1016. https://doi.org/10.1007/s00289-011-0474-3.

15. page 11. Figure 2: Proper SEM (Scanning electron microscopy) images should be provided. SEM images should allow the visualization of surface and its topography/ rugosity. Please replace the images presented by suitable SEM images that are in accordance with results and discussion on porosity.

- The best possible SEM images obtainable from our equipment have been used and updated in the manuscript.

16. page 12. Figure 3: The authors should improve the FTIR spectra regarding band identification. Some vertical lines are included where there are no peak apex, please correct. Discussion should be improved by mentioning the peaks of each component that assures its presence in the final formulation (i.e. PVA/ %1 v/v AuNP / %10 w/v AMP).

- Yes, the following has been corrected in line with the reviewer's comment.

17. page 14 and 15. A joined discussion on metabolic activity and cell viability could be

performed. Are results in agreement?... Section of "MTT assay" and "Fluorescence Microscopy Analyses" should be removed and the focus should be on assay response (Metabolic activity and viability) and not on assay name. In the MTT assay a control of TCPS is used. Please explain the origin/ composition of this control. Figure 5 and Figure 6 could be joined and captions should be improved: for example "Metabolic activity and viability of NNNNN cells exposed to XXXX, YYYY, and ZZZ". TCPS was used as ……." page 16 and 17. Also here the focus should be on osteoblastic differentiation /osteogenic differentiation. Please replace : Section of "ALP Activity" and "Alizarin Red Staining".

- Yes, the results are consistent and have been merged (Figure 5). MTT assay results showed that PVA + 1% AuNP + 1% AMP composition possessed higher metabolic activity as compared to PVA only. The fluorescence microscopy analysis results also confirmed the findings of the MTT data, showing that PVA + 1% AuNP + 1% AMP supported higher cell viability as compared to PVA only.

Overall, significantly enhanced metabolic activity and cell viability occurred in PVA + 1% AuNP + 1% AMP group as compared to PVA only. Based on the MTT assay and fluorescence microscopy results, it was shown that PVA + 1% AuNP + 1% AMP increased its metabolic activity and viability compared to PVA.

The control group was TCPS for each experiment. Exponentially growing cells were plated in flat-bottomed 96-well plates (Corning®, U.S.A.) at 5 x 10^4 cells/well. Culture medium was added in serial dilution to give a final volume of 200 µl/well with TCPS was simulated with the addition of 10% (v/v) fetal bovine serum (FBS) (Sigma-Aldrich, U.S.A.) to the seeding culture medium.

18. Please state clearly the conclusion on the presented work .

- The conclusion has been revised.

Reviewer 4

The authors introduce the antibacterial 3D printed bio-composites of PVA/gold nanoparticles for orthopedic applications. Gold nanoparticles are widely used in diagnosis, drug delivery, biomedical imaging, and photo-thermal therapy due to surface plasmon resonance, fluorescence, and easy surface functionality. After carefully going through this manuscript, I found that it is a very interesting work with promising results, and the evidences the authors provided can well support their results. The structure of this work is well organized with a clear logic, but some parts need to be further improved to make the statements be more suitable, and the figure works in this work should be considerably improved. Based on these concerns, I think a major revision is needed before publishing in this journal, and my comments listed below may help the authors further improve their work:

1. **In the abstract, PVA, AMP, and 3D should be spelled.**

- The aforementioned abbreviations have been spelled in the abstract.

2. **The summary of the progress and current challenge of bio-composites in the introduction part needs further improvement. A few references (Chemistry of Materials 2020 32 (5), 2180-2193) are suggested to include and please be careful to avoid a bias citation.**

- The introduction part has been revised and the appropriate references cited in text.

3. **Why you want to focus on the antibacterial 3D printed bio-composites of PVA/gold nanoparticles for orthopedic applications should be clearly claimed in the end of the introduction part.**

- The following paragraph has been added in the end of the introduction part –

"As discussed above, the complexity of the bone structure and the high destruction caused by bone injuries often leads to complications in bone healing. Here, the application of bespoke bone substitutes will be useful in terms of providing a patient-specific and defect-specific support to restore the original properties of the injured bone tissue. In addition, to combat post-surgical infections, which are either implant-associated contaminations, hospital-led or systemic bacterial invasion from other sites, the innovative concept of surgical implantation of osteogenic-inducing scaffolds with appropriate porosity combined with an antibacterial activity, can provide a more efficient strategy for the regeneration of elective bone defects [23]. Thus the novelty of our work lies in the fabrication of PVA-based 3D printed composites, reinforced with AuNPs and AMP, to develop multi-functional biomaterials for orthopedic applications, with the following objectives: (1) 3D printed PVA-based scaffolds for the production of bespoke surgical implants for orthopedic applications, (2) Incorporation of AuNPs to promote bone cell proliferation and differentiation, mechanical strength, electrophysiological signaling, and antioxidant activity similar to physiological bone tissue, and (3) Addition of AMP to administer anti-bacterial properties to the implants to combat post-implantation infections."

4. The errors shown in Table 1 is high for strain. Why?

- Thank you for this information. There were mistakes on errors. Calculations were performed again and the errors were corrected.

5. The description of Fig 3 and Fig 4 should be further improved.

- The figures have been added in color in the revised manuscript. Also, as per the reviewer's comments above, to bring a better context for the discussion of the data, some of the Figures

have been merged together (Figure 5: MTT and fluorescence microscopy and Figure 6: ALP acitivity and Alizarin Red staining).

6. The figures of this work should be considerably improved. Please avoid using just black-white figures which are not appealing. The logic of the figures should be also improved.

- As suggested by the reviewer, we have added colored graphs for Figures 5, 6 and 7.

7. The conclusion part should be revised to make the highlights be clearer.

- As per the suggestion of the reviewer, the conclusion part was revised.

8. Please carefully check and revise the mistakes found in the reference bibliography.

- We have updated the reference bibliography.

Study on the cytocompatibility, mechanical and antimicrobial properties of 3D printed composite scaffolds based on PVA/ Gold nanoparticles (AuNP)/ Ampicillin (AMP) for bone tissue engineering

Aysenur Topsakal[1,2], Swati Midha[3,4], Esra Yuca[5], Arı Tukay[6], Hilal Turkoglu Sasmazel[6], Deepak M. Kalaskar[3*], Oguzhan Gunduz[1,2,*]

[1] Center for Nanotechnology and Biomaterials Application and Research (NBUAM), Marmara University, 34722, Istanbul, Turkey

[2] Department of Metallurgical and Materials Engineering, Faculty of Technology, Marmara University, 34722, Istanbul, Turkey

[3] UCL Division of Surgery and Interventional Science, Royal Free Hospital Campus, University College London, Rowland Hill Street, NW3 2PF, UK

[4] Special Centre for Nanoscience, Jawaharlal Nehru University, New Delhi-110067, India

[5] Department of Molecular Biology and Genetic Engineering, Yildiz Technical University, Istanbul, Turkey

[6] Metallurgical and Materials Engineering Department, Faculty of Engineering, Atilim University, Incek, 06830, Ankara, Turkey

Corresponding Authors

*Dr. Oguzhan Gunduz: ucemogu@ucl.ac.uk (O.G.).

*Dr. Deepak M. Kalaskar: d.kalaskar@ucl.ac.uk (D.M.K.)

Abstract

Over the years, gold nanoparticles (AuNP) have been widely used in several biomedical applications related to the diagnosis, drug delivery, bio-imaging, photo-thermal therapy and regenerative medicine, owing to their unique features such as surface plasmon resonance, fluorescence and easy surface functionality. Recent studies showed that gold nanoparticles display positive effect on osteogenic differentiation. In line with this effect, 3-Dimesional (3D) scaffolds that can be used in bone tissue were produced by exploiting the properties of gold nanoparticles that increase biocompatibility and support bone tissue development. In addition, ampicillin was added to the scaffolds containing gold nanoparticles as a model drug to improve its antimicrobial properties. The scaffolds were produced as composites of polyvinyl alcohol (PVA) main matrix as PVA, PVA/AuNP, PVA/Ampicillin (AMP) and PVA/AuNP/AMP. Scanning Electron Microscopy (SEM) Fourier Transform Infrared Spectroscopy (FTIR), tensile measurement tests, and *in vitro* applications of 3D scaffolds were performed. As depicted by SEM, scaffolds were produced at pore sizes appropriate for bone tissue regeneration. According to FTIR results, there was no modification observed in the AMP, PVA and gold nanoparticles due to mixing in the resultant scaffolds. *In vitro* results show that 3D printed composite scaffold based on PVA/AuNP/AMP are biocompatible, osteo-inductive and exhibit antimicrobial properties, compared to PVA scaffolds. This study has implications for addressing infections during orthopedic surgeries. The PVA-based gold nanoparticle 3D tissue scaffold study containing ampicillin covers a new study compared to other articles based on gold nanoparticles.

Keywords: gold nanoparticle, PVA, ampicillin, 3D printing, bone tissue engineering

1. Introduction

Three-dimensional printing (3DP), which is of great interest as a promising tool to custom print bone implants has recently been widely used in orthopedics and dentistry [1,2]. When 3DP techniques are compared with the traditional scaffold manufacturing systems, the 3DP is able

to reconstruct critical-sized bone defects with remarkedly higher strength and porosities [3]. Use of patients own X-ray computed tomography (CT) images makes 3DP very useful for generating patient-specific and defect-specific implants [4]. With the help of CT based 3D reconstructed images, biomimetic 3D scaffolds can be put into production with the help of computer aided design (CAD) and computer aided production systems [5]. The controlled delivery of bioactive substances and drugs to the bone is an area of intensive research aimed at designing distribution platforms that can have a therapeutic role on bone diseases such as infection or cancer, with the activation of bone regeneration processes. Among them, 3D structures can provide a temporary framework that provides a favorable environment for cell adhesion and growth and thus can aid bone regeneration. It also provides a valuable platform for local on-site influences or delivery strategies [6]. Polyvinyl alcohol (PVA) has been used in numerous medical applications, including drug delivery systems, wound dressings, and even soft touch lenses. This water-soluble synthetic polymer is not just biocompatible, biodegradable, and nontoxic, but it also provides sufficient mechanical strength and flexibility to the scaffolds. However, PVA has a tendency to be resistant to protein absorption and cell adhesion because of the lack of bioactive components [7].

In last few years, the interest in using osteoconductive or inductive agents to improve bone tissue regeneration has increased [8–11]. For the successful localized delivery system of osteogenic agents, the agent must be kept in the defective area of bone defect for the required time to achieve targeted treatment [11,12]. Among the several types of micro- and nano carriers used as biomolecule delivery agents, gold nanoparticles (AuNPs), are very attractive materials for systemic delivery [13,14]. It has many features of itself such as non-cytotoxicity, ease of preparation with defined sizes, reproducibility, and easy surface modification with various thiol-containing biomolecules through gold–thiol bonding [15]. Especially, AuNPs show effect on

bone remodeling by enhancing the osteogenic differentiation by inhibiting the osteoclast activity. This effect makes that the AuNPs very promising materials for applications in bone tissue regeneration [16,17].

At the beginning of the 21st century, post-surgical orthopedic infections developed rapidly due to the correct use of antibiotics and disinfection in hospital facilities. According to the National Institutes of Health (NIH), around 100,000 people die as a result of infections in the US, which means an average of 300 deaths a day. One of the new strategies developed to combat this rapid increase in bacterial infections is by leveraging the advantages of nanotechnology [18]. However, despite imparting superior osteogenic regeneration in the bone defect sites, orthopedic implants are highly prone to post-surgical infections, causing severe complications in patients, and in some cases, even morbidity [19]. To avoid these complications, scaffolds loaded with either antibiotics [20,21] or antimicrobial nanoparticles [19] are being heavily researched in laboratories. The local administration and delivery of antibiotics directly on the site of infection seems like a logical approach, as it allows overcoming the side-effects of indirect delivery methods with significant reduction in antibiotic dosage [22] or this purpose, the use of broad-spectrum antibiotics like ampicillin, which is highly compatible with several tissue engineered bone substitutes [23,24], is extremely promising for achieving a successful and infection-free regeneration of the injured bone region in patients.

As discussed above, the complexity of the bone structure and the high destruction caused by bone injuries often leads to complications in bone healing. Here, the application of bespoke bone substitutes will be useful in terms of providing a patient-specific and defect-specific support to restore the original properties of the injured bone tissue. In addition, to combat post-surgical infections, which are either implant-associated contaminations, hospital-led or systemic bacterial invasion from other sites, the innovative concept of surgical implantation of

osteogenic-inducing scaffolds with appropriate porosity combined with an antibacterial activity, can provide a more efficient strategy for the regeneration of elective bone defects [25]. Thus the novelty of our work lies in the fabrication of PVA-based 3D printed composites, reinforced with AuNPs and AMP, to develop multi-functional biomaterials for orthopaedic applications, with the following objectives: (1) 3D printed PVA-based scaffolds for the production of bespoke surgical implants for orthopaedic applications, (2) Incorporation of AuNPs to promote bone cell proliferation and differentiation, mechanical strength, electrophysiological signalling, and antioxidant activity similar to physiological bone tissue, and (3) Addition of AMP to administer anti-bacterial properties to the implants to combat post-implantation infections.

2. Materials and Methods

2.1 Scaffold fabrication

PVA solution was prepared by dissolving PVA at 13% w/v in distilled water. PVA solution was printed using custom modified (Ultimaker^{2+}) as extrusion printer and the most suitable production for scaffolding production was selected and optimized as showed in Figure 1. 4 different groups were formed: Group 1: containing 80 nm AuNPs (1.1 particles/mL) in PVA solution. While preparing a 13 w/v% PVA solution, 1 mL of (80 nm) AuNP were added into 10 mL. Group 2: PVA solution containing 10 mg AMP. Group 3: containing AuNP (80 nm) and AMP in 13% w/v PVA solution. 1 ml of (80 nm) AuNP and 10 mg/mL AMP were added to the PVA solution (13% w/v). Before the writing process, a rectangular prism of 20x20x3mm was drawn using the SolidWorks design program. In line with the features expected from the tissue scaffold, besides design controls such as occupancy rate, number of layers, shape and angle; With the Simplify program, which enables the control of process parameters such as speed, temperature and flow rate, a tissue scaffold with a height of 10 times (0.35mm) at +45, -45 angles and 85% fullness was prepared, and pre-printing controls were made on the simulation screen of the program. Subsequently, the design was transformed into a G-Code that the

bioprinter could perceive, and made ready for writing. The tissue scaffolds were produced at room temperature at an optimized flow rate of 0.5 mL / h using a needle with an outer diameter of 0.5 mm and an inner diameter of 0.3 mm.

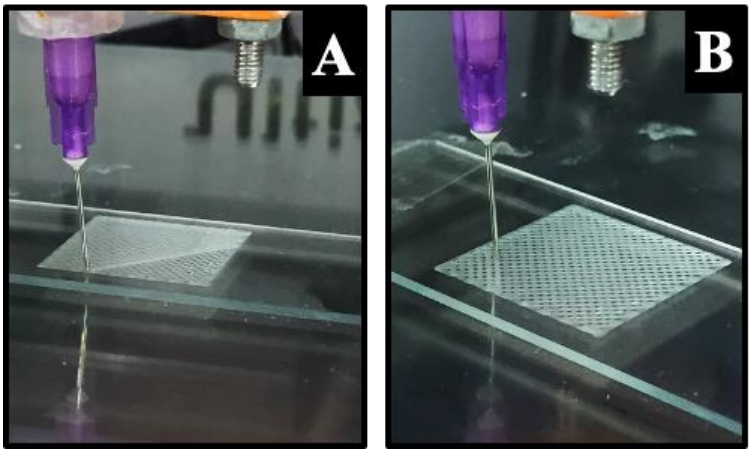

Fig. 1. Production of PVA based scaffolds by 3D printing method.

2.3 Characterization of 3D printed composite scaffolds

2.3.1 Mechanical Characterization

The mechanical properties of the resultant scaffolds were obtained by measuring tensile strength (Shimadzu EZ-LX) at room temperature (23°C) and at a speed set at 5 mm / min. The resultant thickness of the scaffolds post-printing was analyzed by digital micrometer (293-100, Mitutoyo, Japan).

2.3.2 Morphological analysis

Morphological and topographical details of 3D mats (PVA, PVA/AuNP, PVA/AMP and PVA/AuNP/AMP) were analyzed by Scanning Electron Microscopy (SEM) (EVA MA 10, ZEISS, USA) post sputter coating with Au/Pl for 60 seconds.

2.3.3 Chemical structure analysis

The chemical structures of PVA, PVA/AuNP, PVA/AMP, PVA/AuNP/AMP scaffolds were analyzed by Fourier Transform Infrared Spectroscopy (FTIR, Jasco, FTIR 4700). Infrared spectra were recorded within 500 - 4000 cm^{-1} wavelength region with a Gladi attenuated total reflection (ATR) imaging plate (Diamond ATR crystal) and a spectrometer (Jasco, FT/IR 4700) equipped with liquid nitrogen-cooled mercury cadmium telluride (MCT) detector.

2.3.4 XRD analysis

X-ray diffraction analysis was performed using X-Ray diffraction device (SHIMADZU XRD-6100) to observe the crystal structures of AuNP in PVA/AuNP and PVA/AuNP/AMP scaffolds. The sample was ground and pressed into the sample holder to obtain a smooth plane surface, and the diffraction pattern was recorded in the range of 2θ between 10° to 80°.

2.3.5 Cell Culture Studies

For cell culture studies, MC3T3-E1 mouse osteoblast cells were obtained from Department of Bioengineering, Kirikkale University (Kirikkale, Turkey). DMEM/F-12 (Dulbecco's Modified Eagle Medium/Nutrient Mixture F-12), FBS (fetal bovine serum), L-glutamine, penicillin/streptomycin, BSA (bovine serum albumin) and Phosphate buffer saline (PBS) tablets were bought from Amresco (Solon, U.S.A.). Ethanol (99% purity, vol./vol.), 3-(4,5-dimethyl-2-thiazol)-2,5-diphenyl-2H-tetrazolium bromide (MTT) powder, Trypsin/EDTA solution at 0.25 % (w./v.), Triton X-100, glutaraldehyde, dimethylsulfoxide (DMSO), hexamethyldisilane (HMDS) (99% purity, vol./vol.), BCIP/NBT tablets were bought from Sigma-Aldrich (St. Louis, U.S.A.). Additionally, the stains 4,6-diamidino-2-phenylindole Dihydrochloride (DAPI), Alizarin Red-S and Alkaline Phosphates (ALP) kits were bought from Sigma-Aldrich (St. Louis, U.S.A.).

Cell culture studies were performed by using MC3T3-E1 mouse osteoblast cell line to biological characterization of the 3D printed PVA, PVA + 1 wt. % AuNP, PVA + 1 wt. % AMP, PVA

+ 1 wt. % AuNP + 1 wt. % AMP mats. The 3D printed mats were cut as circular shapes with 5 mm diameters and 0.2 mm thicknesses and sterilized under UV for 45 minutes. The samples were placed into 96-well plates and MC3T3-E1 cells were seeded onto the prepared scaffolds at a seeding density of 2×10^3 cells/mL and incubated under 5% CO_2 at 37°C for 21 days in culture. DMEM/F-12, FBS (10% v/v), penicillin streptomycin solution (1% v/v) and L-glutamine (1%v/v) was used as the growth medium. Cell viability was determined by MTT Assay, calcium deposition was detected by Alizarin Red Staining, the differentiation was determined by Alkaline Phosphates Activity (ALP); the adhesion, growth and proliferation characteristics of the seeded 3D printed mats were examined by fluorescence microscopy imaging. All assays were done at 21 day. The control group was TCPS for each experiment. Exponentially growing cells were plated in flat-bottomed 96-well plates (Corning®, U.S.A.) at 5 x 10^4 cells/well. Culture medium was added in serial dilution to give a final volume of 200 µl/well with TCPS was simulated with the addition of 10% (v/v) fetal bovine serum (FBS) (Sigma-Aldrich, U.S.A.) to the seeding culture medium. MC3T3-E1 mouse osteoblast cells were obtained from the Department of Bioengineering, Kirikkale University (Kirikkale, Turkey).

MTT Assay

MTT assay was performed to study the cell viability of osteoblast MC3T3-E1 cells on 3D printed samples on days 1st, 7th, 14th, and 21st day. After the incubation session (37 °C, 5% CO_2), the cell culture media was removed, and samples were rinsed with PBS solution with three times. After washing the samples, 90 µL fresh medium and 10 µL MTT solution (Sigma-Aldrich, U.S.A.) were added into the each well and incubated for an additional 3 hours. After incubation period, the MTT solution was discarded, and the formazan crystals were dissolved in 200 µL DMSO (Sigma-Aldrich, U.S.A.) and incubated for 1 hour. Finally, the media from the wells were taken and the absorbance values of the solution were measured by Dynamica LEDETECT96 microplate reader at 540 nm [26].

Fluorescence Microscopy Analyses

Fluorescence microscopy analysis were done to observe cell attachment and growth on/within the developed 3D printed scaffolds. The microscopy images were taken on the 7th, 14th and 21st days of the cultivation. The cultured samples were removed from the incubator and after discarding the medium the samples were washed three times with PBS. To increase cellular permeability, the samples were immersed in 0.1% Triton X-100 solution (Sigma-Aldrich, U.S.A.) for 5 minutes, followed by PBS washing. The cells on the 3D printed scaffolds were stained with 10 mg/mL DAPI solution (Sigma-Aldrich, U.S.A.) and kept in the dark at room temperature for 15 minutes. Finally, the images were taken with using Fluorescent Microscope (AMG EVOS-FL, U.S.A.) [26].

ALP Activity

The ALP activity of the cultured 3D printed mats was examined on the 7th, 14th and 21st days of the cultivation. Originally, nitro blue tetrazolium and 5-Bromo-4-Chloro-3-Indolyl Phosphate (NBT/BCIP) tablet (Sigma-Aldrich, U.S.A.) was dissolved in 10 mL distilled water (dH_2O) to form the substrate solution. Prepared substrate solution was stored in dark at room temperature for 2 hours. The cultured samples were removed from the incubator, the medium was gently discarded, and the cells were washed with PBS for three times. Afterwards, samples were submerged in 10% formalin solution (Sigma-Aldrich, U.S.A.) and left for maximum 60 seconds. After the removal of formalin solution, the samples were washed with PBS for three times. Substrate solution was added to the wells, incubated at room temperature for 10 minutes and the measurements were taken at 405 nm.

Alizarin Red Staining

Alizarin Red staining (Sigma-Aldrich, U.S.A.) was performed for observing calcium deposition in the cell seeded mats. 2 g of Alizarin Red satin was dissolved in 10 mL dH_2O and pH of the solution was strictly adapted to 4.1-4.3 using HCl. The resultant solution was stored in the dark

until use. The scaffolds pre-incubated with cells were washed with PBS. Thereafter, 10% formalin was added into the wells for 30 minutes to fix the cells. Formalin was carefully discarded; the cells were washed with dH_2O and stain solution was added on the samples. Then they were incubated in the dark at room temperature for 30 minutes. Samples were then centrifuged at 200 rpm. Lastly, the absorbance values of the respective solutions were measured at 405 nm from the microplate reader to determine level of calcium deposition or mineralization [27].

2.3.5 Antimicrobial Activity Assay

Gram positive bacteria *S. aureus* was used to test antimicrobial activity of the samples. S. aureus (ATCC 25923) was used for antibacterial analysis. The bacterial culture was cultivated in Luria-Bertani (LB) broth (10 g/L bacto-tryptone, 5 g/L yeast extract, 5 g/L NaCl) overnight at 37 °C. 10^7 colony-forming units (CFU/mL) were inoculated on LB-agar plate. The scaffolds were gently placed on the bacteria inoculated agar plates and incubated at 37 °C for 24h. The diameter of the inhibition zone around each scaffold sample was measured using a ruler.

Statistical Analysis

All experiments were done in triplicate data sets (N=3). Two-way analysis of variance (ANOVA) conducted with Tuckey's multiple comparisons test was conducted to determine the statistical differences, using GraphPad prism v8.0 software. For all results, $p < 0.05$ was accepted as statistically significant.

3. Results and Discussion

3.1 3D printing of composite scaffolds

Optimum concentration of the composites (10% w/v PVA, 13% w/v PVA and 15% w/v PVA) was determined for printing. One of the important factors is that the layers in a 3D printed scaffold are continuous, smooth and uninterrupted. During ink optimization, we experienced

spreading of the layers resulting in clogging of pores using 10% w/v PVA solution. In 3D printing using 15% w/v PVA solution, the layers were discontinuous. The most suitable concentration for 3D printing was found to be 13% w/v PVA. At this concentration, the layers were straight, uninterrupted and the pores were uniformly distributed. Pore size distribution of scaffolds and properties of layers were not affected by the addition of AMP and AuNP. Final produced scaffold has 20x20mm dimensions and about 0.35 mm height. This information has now been added to the results section.

Polyvinyl alcohol (PVA) is a water-soluble synthetic polymer widely used in biomedical applications [28–30], as a 3D printed polymer and drug carrier, owing to its excellent biocompatibility. Using FDM-based 3D printing, filaments of PVA containing drugs have been fabricated with specific release profiles [31,32]. However, with the elevated temperatures used for extrusion in FDM-based printing, producing scaffolds with thermolabile drugs is often a big limitation. Our custom modified extrusion printer addresses the above issue by enabling printing at room temperature, and hence could be used for upscaling pharmaceutical applications of 3D printed PVA.

3.2 Characterization of 3D scaffolds

Table 1. Mechanical test of the scaffolds

Scaffold Structure	Stress (MPa)	Strain (%)
Pure %13 w/v PVA	0,13±0,0074	72,38±7,46
PVA/ %1 v/v AuNP	0,187±0,135	78,01±6,84
PVA/ %10 w/v AMP	0,183±0,0228	98,02±6,79
PVA/ %1 v/v AuNP / %10 w/v AMP	0,162±0,137	66,61±5,43

The average values and standard deviations of tensile strength and tensile fracture of PVA, PVA/AMP, PVA/AuNP and PVA/AMP/AuNP tissue scaffolds are shown in Table 1. While

the tensile strength of pure PVA scaffold was 0,13±0,0074 MPa, the tensile strength values of PVA/AuNP and PVA/AMP scaffolds were 0.187±0.135 MPa and 0,183±0,02 MPa, respectively. The incorporation of AuNP into the tissue skeleton resulted in an increase in the tensile strength of the skeletons [14]. Merchan et al. has reported the effect of increasing antibiotics on the mechanical properties. However, the presence of AMP influences tensile strain and tensile strength significantly. In case of AMP, the effect of its presence in the systems on Young's modulus is hardly noticeable in the investigated range of the antibiotic (up to 1 wt.%). The authors showed that the former mentioned tensile characteristic is reduced at 1 wt.% presence of AMP [33].

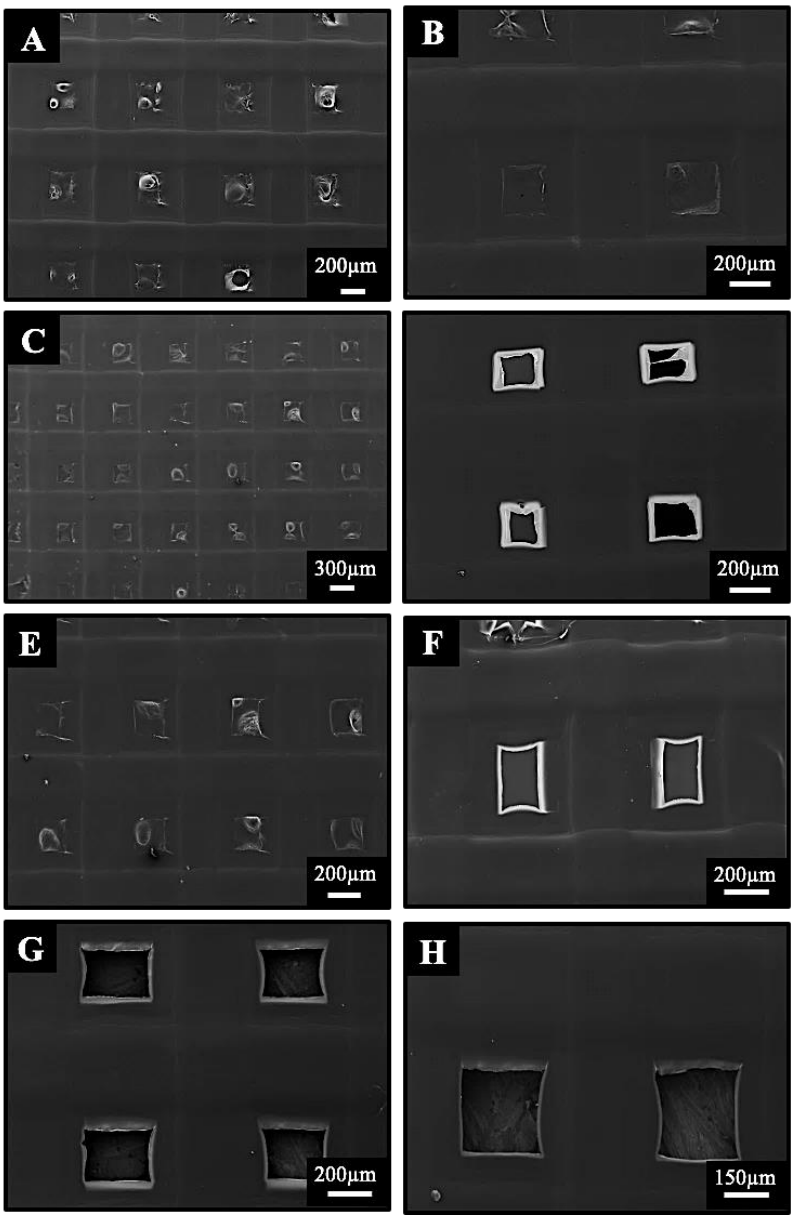

Fig. 2. SEM images of (A, B) pure PVA, (C, D) PVA/AuNP, (E, F) PVA/AMP, (G, H) PVA/AuNP/AMP scaffold samples.

Porosity is defined as the percentage of void spacing in a solid and is a material-independent morphological feature. Pores are required for bone tissue formation because they promote the migration and proliferation of osteoblasts and mesenchymal cells, as well as vascularization. A porous surface improves the mechanical coupling between the implant biomaterial and the surrounding natural bone, providing greater mechanical stability at this critical interface. The SEM

images taken to observe the morphological structures, pore structure and pore sizes of the produced 3D tissue scaffolds are shown in Figure 2. The 3D printed scaffold contained open and uniform interconnected pores to enable the supply of nutrients, oxygen, and other molecules to the scaffold core and to facilitate cell growth [34,35]. The pores in the 3D scaffold structures were evenly distributed, with pore sizes of approximately ~ 300 microns. The minimum requirement for pore size is considered to be about 100 microns to facilitate cell migration, and transport of nutrients [34]. Pore size is an important parameter determining vascularization, and hence affecting the progression of osteogenesis. Small pores support hypoxic conditions and produce osteochondral tissue formation induced before osteogenesis, while well vascularized large pores directly lead to osteogenesis. However, it is known that pore sizes greater than 300 micrometers are the optimal pore size for bone tissue scaffold applications due to new bone formation and formation of capillaries [36].

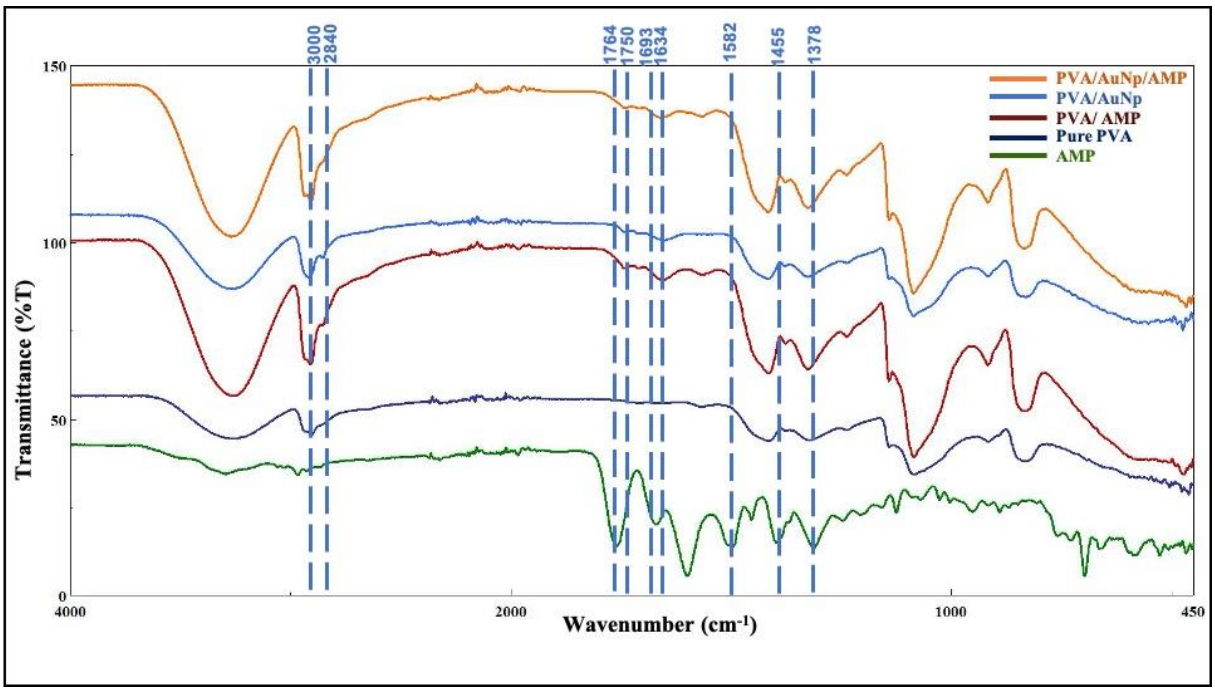

Fig. 3. FTIR spectra of ampicillin, pure PVA, PVA/AMP scaffold, PVA/AuNP scaffold, PVA/AuNP/AMP scaffold.

The chemical structure of the tissue scaffolds and the chemical interactions in the material were revealed using FTIR. The FTIR data for PVA, PVA/AMP, PVA/AuNP and PVA/AuNP/AMP

scaffolds showing the chemical structures are shown in Figure 3. As the main matrix of scaffolds was PVA, the peak values of PVA were dominant and displayed dense peaks. All major peaks related to hydroxyl and acetate groups were observed. Large bands observed between 3550 and 3200 cm^{-1} bind to O-H extending from intermolecular and intramolecular hydrogen bonds. The vibration band observed between 2840 and 3000 cm^{-1} corresponds to stretching C-H from alkyl groups, and peaks between 1750-1735 cm^{-1} are caused by stretching of C = O and C-O from the acetate group remaining from PVA [37,38]. After incorporating into the PVA matrix, because of the absence of the signal in the region of 1764 cm^{-1} in PVA spectrum, there is a flattening of the peaks in this region. An absence of a signal in the region of 1700 cm^{-1} indicates that only a small amount of acetate groups can be present in the polymer chain as the used PVA is highly hydrolyzed [39]. The broadband at about 3276 to 3337 cm^{-1} indicates the presence of OH group hydroxides in AuNP. The apparent peak at 1634 and 1636 cm^{-1} is due to gold nanoparticles [40]. When we consider the peak values of AMP drug, the peak values of 1764 cm^{-1} and 1693 cm^{-1}, respectively, the beta-lactam ring and amide bond to -C = O, 1640 cm^{-1} and 1378 cm^{-1} peak values symmetrical and asymmetric -COOH. Finally, the peaks at 1582 cm^{-1}, 1525 cm^{-1} and 1455 cm^{-1} are divided into N-H deformation of the amide bond, -NH2 bending, and -C = C-C stretching of the aromatic ring, respectively [41]. By virtue of no other modifications in the spectra, it is plausible to infer that no chemical interactions are occurred between PVA and AuNP with AMP, which might imply that the antibiotic can be released from the matrix and even that the structure does not suffer significant modifications and no alterations on the antibacterial activity of AMP whatsoever. Similar pattern is evidenced in the spectra for PVA/AMP as well as PVA/AuNP/AMP samples.

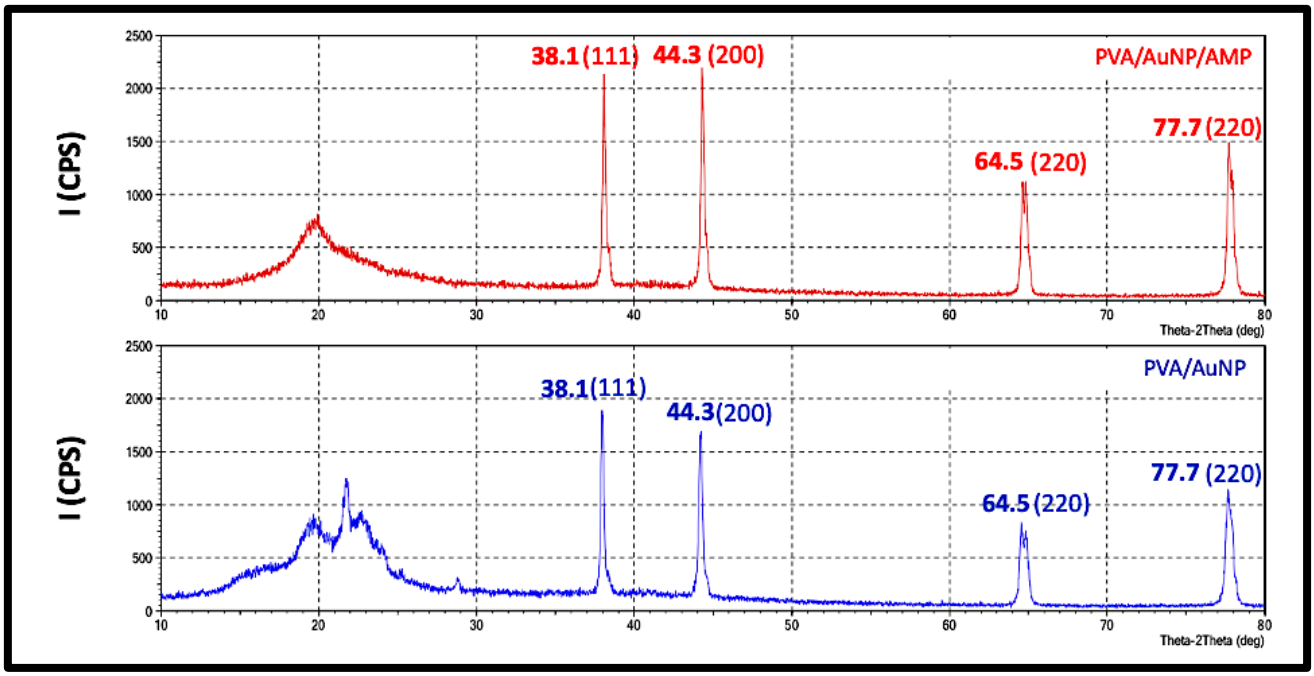

Fig. 4. XRD analysis of PVA/AuNP/AMP and PVA/AuNP scaffold samples. Crystalline nanoparticles represented by four peaks corresponding to standard Bragg reflections (111), (200), (220), and (311) of face centers cubic lattice.

The crystallinity of the synthesized AuNPs was determined by XRD technique and the corresponding XRD patterns are shown in Figure 4. Gold nanocrystals showed four separate peaks at 2θ = 38.1, 44.3, 64.5 and 77.7. All four peaks were found to correspond to the standard Bragg reflections 111, 200, 220 and 311 of the face center cubic lattice. The peak diffraction at peak 38.1 shows that the preferred growth orientation of gold is fixed in the direction. This corresponds to solids of molecular size formed by a repeating 3D atom model or molecule having an equal distance between each part [42].

3.4 Cell Culture Studies

Metabolic Activity and Viability

The metabolic activity of MC3T3-E1 cells on the prepared 3D printed mats up to 21 days is shown in (Figure 5-A). The prepared 3D printed mats did not exhibit any toxic effects on the osteoblast cells for 21 days. At day 21, all the 3D printed mats exhibited significantly high cell viability as compared to TCPS ($p<0.0001$ for all groups). Therefore, it is safe to assume that

this is, indeed, a result of the framework of the fabricated 3D printed mats offering a more suitable, porous microenvironment for the cells, as compared with the 2D TCPS. As seen in the fluorescence microscopy data (Figure 5-B), PVA + 1% AuNP, PVA + 1% AMP and PVA + 1% AuNP + 1% AMP mats showed the higher viability as compared PVA only. The fluorescence microscopy analysis was performed to investigate cell attachment, distribution and viability on the 3D printed mats on the 7^{th}, 14^{th} and 21^{st} days of the cultivation period (Figure 5-B). It was observed that the cell viability and cell attachment and viability were increased for all type of the samples overtime, as compared to TCPS control, suggesting good cytocompatibility of the scaffolds.

Cytotoxicity of AuNPs in human cells is size/shape, concentration and time dependent, and is known to promote cell proliferation as well as osteoblastic differentiation significantly in certain sizes and concentrations [43]. Using a similar cell line model (MC3T3-E1), Singh et al. reportedly demonstrated proliferative and osteoinductive effect of gold nanoparticles, both *in vitro* and *in vivo* [44]. In a recent study, Zhang et al. demonstrated that gold nanoparticles not only stimulated the cell proliferation of bone progenitors in vitro, but also aided in the expression of osteogenic biomarkers. The extent of this AuNP-induced osteogenesis increased with increasing size of the nanoparticles, reporting highest mineral formation at 45 nm AuNP dimensions [45]. Furthermore, our cell viability was not affected by ampicillin loaded mats (PVA + 1% AMP and PVA + 1% AuNP + 1% AMP) exhibited significantly higher cell viability compared to the PVA mats at days 7, 14 and 21 respectively ($p<0.001$). This result is in accordance with previous studies where the scaffold properties, such as morphology, surface chemistry, composition and pore architecture predominantly dictate cellular behavior, reporting no adverse effect from the antibiotics loaded in the scaffolds [46]. Customizing the filament diameters of 3D printed scaffolds have been used as an efficient way to regulate the release rate of antibiotic drugs by some studies [47].

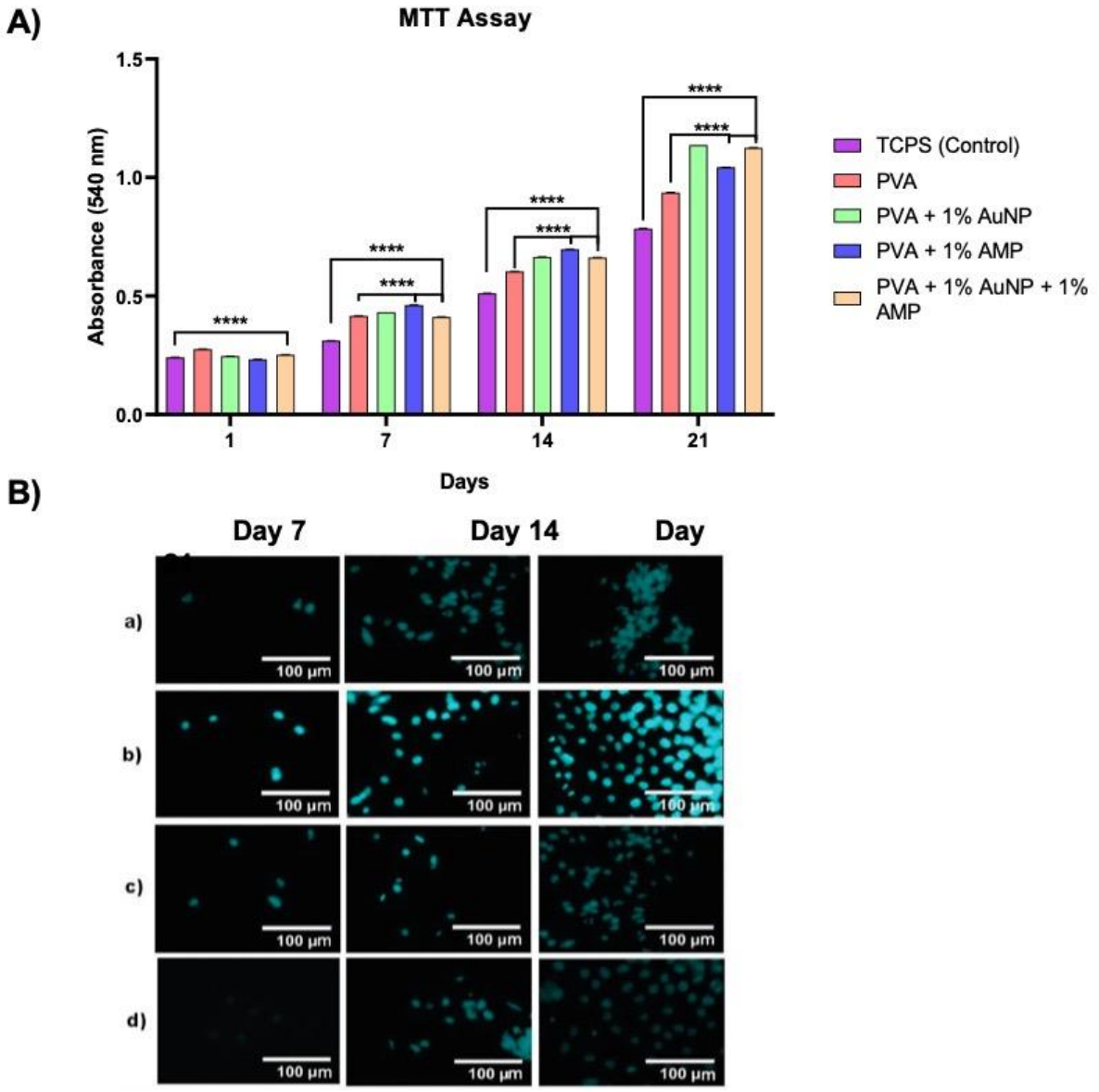

Fig. 5. Metabolic activity and viability of MC3T3-E1 cells cultured on PVA, PVA+%1AuNP, PVA+%1AMP AND PVA+%1AuNP+%1AMP. TCPS was used as the 2D control in the study. A) MTT bar graph with absorbance values (for experimental and control groups) plotted against the time of culture. Statistical significance 'p' is represented as, $p<0.05$ = '*', $p<0.01$ = '**', $p<0.001$ = '***', $p<0.0001$ = '****'.

B) Fluorescence micrographs of a) PVA, **b)** PVA + 1% AuNP, **c)** PVA + 1% AMP, **d)** PVA + 1% AuNP + 1% AMP, on 7th, 14th and 21st days of cultivation period. All images are taken with x40 magnification. Scale bars = 100 µm.

Overall, significantly enhanced metabolic activity and cell viability occurred positively in PVA + 1% AuNP + 1% AMP group as compared to PVA only.

Osteoblastic and Osteogenic Differentiation

ALP activity is an important parameter to confirm early osteoblastic differentiation which accumulates inorganic phosphate [1]. The results of the ALP activity of the MC3T3-E1 laden 3D printed PVA mats, PVA + 1% AuNP, PVA + 1% AMP and PVA + 1% AuNP + 1% AMP mats are shown in Figure 7 as a (%) change after 7^{th}, 14^{th} and 21^{st} day of culture. In terms of ALP activity, the cells favored the 3D printed mats compared to the TCPS. The reason behind that could be the porous, hydrophilic structure of the 3D printed mats that is crucial for the osteogenic response [1]. The highest ALP activity was observed for PVA +1% AuNP and PVA 1% AuNP + 1% AMP mats are shown in (Figure 6-A) as compared to PVA only ($p<0.0001$), at all-time points tested. This is could be due to the ability of AuNPs to activate the ERK/MAPK signaling pathway which is responsible for the proliferation and differentiation of a variety of cells systems, including osteoblasts [48,49]

Mineralization is the final stage in the process of osteogenic differentiation. Typically, when the cells start to mineralize, calcium depositions are formed as an indicator of mature cellular differentiation. At 7^{th}, 14^{th} and 21^{st} day of culture, extracellular calcium deposition in TCPS, PVA, PVA + 1% AuNP, PVA + 1% AMP and PVA + 1% AuNP + 1% AMP mats were measured by Alizarin Red Staining. As shown in (Figure 6-B), a similar trend in the staining pattern was observed as seen in the MTT (Figure 5-A) and ALP activity (Figure 6-B), all of the 3D printed mats showed significantly higher mineralization than TCPS ($p<0.001$) at all time points tested. According to the results, highest mineralization levels were found for PVA + 1% AuNP over PVA + 1% AuNP +1% AMP mats at days 14 ($p<0.0001$) and 21 ($p<0.0001$) respectively. Using 60 nm gold nanoparticles, Nah et al. demonstrated osteogenic stimulation in human adipose stem cells using alizarin red and reported similar levels of mineralization (OD.540 value

corresponding to approximately 3) after 21 days of culture [49], as seen in our study. The activation of ERK/MAPK signaling pathway by AuNPs has been identified as a key mechanism for triggering this enhanced osteogenic response [48].

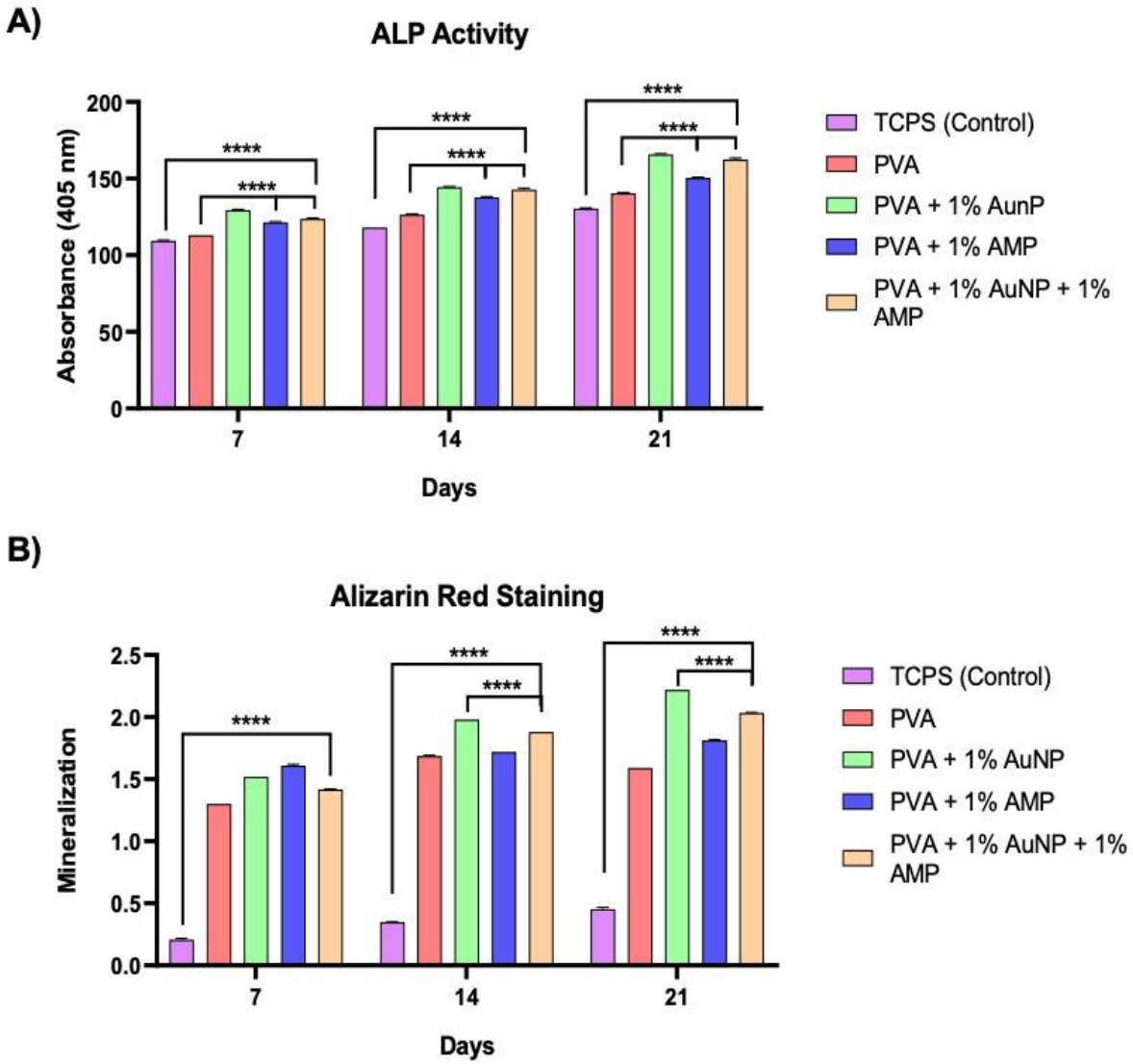

Fig. 6 The extent of osteogenic differentiation in MC3T3-E1 cells cultured on the 3D printed scaffolds detected using early (ALP) and late (Alizarin Red) stage markers of differentiation. TCPS was used as 2D control in the study. A) ALP activity of the MC3T3-E1 cells on 3D printed mats (BCIP tablet was used as blank substrate and its value was accepted as 100). B)

Alizarin Red staining, statistical significance 'p' is represented as, $p<0.05$ = '*', $p<0.01$ = '**', $p<0.001$ = '***', $p<0.0001$ = '****'.

3.5 Antimicrobial Activity of 3D scaffolds

Bacterial growth inhibition was observed for both scaffolds with AMP and AMP+AuNP. PVA only scaffold and AuNP containing scaffold did not show any inhibition zone, implicating no bacterial properties of AuNP alone against S. aureus. PVA/AMP containing scaffolds showed a larger zone of inhibition compared to PVA/AMP/AuNP. This result represents that PVA/AMP/AuNP scaffold retains its antibacterial activity after functionalization with AuNP as shown previously [50]. This may have been, partly, the result of the gold nanoparticles having a slightly reducing effect on AMP activity.

For the antibacterial efficacy of ampicillin, one of the β-lactam antibiotics, the β-lactam ring must remain accessible. Thus, by binding to bacterial transpeptidases, they prevent the covalent cross-linking of peptidoglycans necessary for cell wall construction and growth of bacteria. AuNP-Ampicillin hybrid systems have been the subject of many studies to date and the antibacterial properties of AuNP-Ampicillin conjugates for gram positive and gram negative bacteria have been characterized. In AuNP-Ampicillin hybrids where this type of surface is functionalized, the lactam ring orientation can be adjusted to maintain antibacterial efficacy [51]. In our scaffold system, antibiotics and nanoparticles were added as separate components during scaffold fabrication without being subjected to a conjugation process. As a result of the uncontrolled interactions of free gold nanoparticles and ampicillin molecules in the environment, the orientation of the beta-lactam ring may limit binding with bacterial transpeptidases.

In this study, although a decrease in antibacterial effect was observed with the addition of free AuNP to the scaffold system, we achieved our goal of retaining the antibacterial activity effective in the 3D printed scaffold system even after exposure to UV or the addition of gold nanoparticles in the production process. Elmolla et al. has reported the effects of UV on different

antibiotics. It has been reported that Ampicillin undergoes a 3.8 % degradation after 3 hours of UV application [52]. Another detailed study performed by Naveed et al., further confirmed that UV exposure of 30 mins has minor effect on the degradation of ampicillin and the antibiotic remains within the official limits i.e. 95-105% of the drug should be available in % assay [53]. Based on these previous literature, we applied UV for 45 minutes duration to the scaffold surface, as it would possibly cause very limited amount of degradation of the antibiotic in the scaffolds.

Overall, in the scaffolds developed in this study, AuNP properties that both preserve the antimicrobial property and potentially gain functions such as biocompatibility have been preserved and a multifunctional scaffold has been produced.

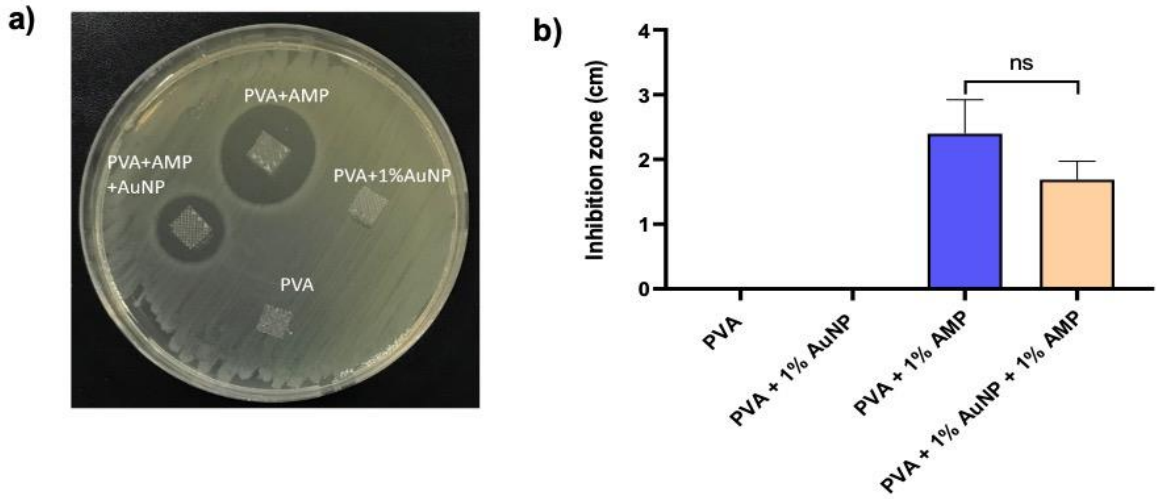

Fig. 7. Inhibition zones of the scaffold samples. a) Representative image of the agar plate for the *S. mutans* agar diffusion test. (b) Graphical representation of inhibition zone diameters to compare PVA, PVA+AuNP, PVA+AMP and PVA+AMP+AuNP scaffold samples. Statistical significance 'ns' denotes 'non-significance'.

In this study, we designed an antibacterial scaffold system and provided proof of concept of increased osteogenic differentiation of the scaffold which could potentially be used as a surgical implant in orthopaedic implantations. Considering the limitations of conjugating antibiotics on the resultant osteogenic differentiation of scaffolds, we used antibiotics and gold nanoparticles

in free form in the system without creating a hybrid structure. In this multifunctional 3D-printed scaffold system, we used Ampicillin as the model antibacterial agent and showed its effect on *S. aureus*, the primary causative agent for osteomyelitis. The system is simple, robust and economical, hence a broad spectrum of other antibiotics such as vancomycin and minocycline could be easily applied to our system to be used against orthopaedic infections.

4. Conclusion

In this study, we have developed 3D scaffolds as bone tissue substitutes, using a unique combination of AuNPs and AMP to accelerate bone tissue formation while providing antimicrobial properties. The scaffolds have been successfully fabricated by advanced 3D printing technique using a homogeneous PVA-based ink comprising of AMP and gold nanoparticles. *In vitro* 3D cell-based assays validated the biocompatible, osteoinductive and antibacterial nature of the PVA/AuNP/AMP scaffolds, thus warranting further screening of the material for clinical translation to treat orthopedic infections by targeted delivery of antibiotics. These findings suggested that the 3D scaffolds may provide an effective treatment strategy against orthopedic infections with concurrent bone formation, a promising view in the design of novel antimicrobial biomaterials potentially suitable for bone tissue engineering applications.

5. Acknowledgment

AT would like to thank funding by BAPKO project, Turkey (FEN-B-121218-0614) for funding this research. DMK would like to thank UKIERI project (547073) for collaborative work. SM is supported by DST project (DST (DST/INSPIRE/04/2017/000645).

6. References

[1] J.J. Li, M. Ebied, J. Xu, H. Zreiqat, Current Approaches to Bone Tissue Engineering: The Interface between Biology and Engineering, Adv. Healthc. Mater. 7 (2018) e1701061. https://doi.org/10.1002/adhm.201701061.

[2] G. Brunello, S. Sivolella, R. Meneghello, L. Ferroni, C. Gardin, A. Piattelli, B. Zavan,

E. Bressan, Powder-based 3D printing for bone tissue engineering, Biotechnol. Adv. 34 (2016) 740–753. https://doi.org/10.1016/j.biotechadv.2016.03.009.

[3] L. Roseti, V. Parisi, M. Petretta, C. Cavallo, G. Desando, I. Bartolotti, B. Grigolo, Scaffolds for Bone Tissue Engineering: State of the art and new perspectives, Mater. Sci. Eng. C. 78 (2017) 1246–1262. https://doi.org/10.1016/j.msec.2017.05.017.

[4] D. Tang, R.S. Tare, L.Y. Yang, D.F. Williams, K.L. Ou, R.O.C. Oreffo, Biofabrication of bone tissue: Approaches, challenges and translation for bone regeneration, Biomaterials. 83 (2016) 363–382. https://doi.org/10.1016/j.biomaterials.2016.01.024.

[5] A. Youssef, S.J. Hollister, P.D. Dalton, Additive manufacturing of polymer melts for implantable medical devices and scaffolds, Biofabrication. 9 (2017) 012002. https://doi.org/10.1088/1758-5090/aa5766.

[6] A.S. Saraiva, I.A.C. Ribeiro, M.H. Fernandes, A.C. Cerdeira, B.J.C. Vieira, J.C. Waerenborgh, L.C.J. Pereira, R. Cláudio, M.J. Carmezim, P. Gomes, L.M. Gonçalves, C.F. Santos, A.F. Bettencourt, 3D-printed platform multi-loaded with bioactive, magnetic nanoparticles and an antibiotic for re-growing bone tissue, Int. J. Pharm. 593 (2021) 120097. https://doi.org/10.1016/j.ijpharm.2020.120097.

[7] H. Kim, G.H. Yang, C.H. Choi, Y.S. Cho, G.H. Kim, Gelatin/PVA scaffolds fabricated using a 3D-printing process employed with a low-temperature plate for hard tissue regeneration: Fabrication and characterizations, Int. J. Biol. Macromol. 120 (2018) 119–127. https://doi.org/10.1016/j.ijbiomac.2018.07.159.

[8] S. Pina, J.M. Oliveira, R.L. Reis, Natural-based nanocomposites for bone tissue engineering and regenerative medicine: A review, Adv. Mater. 27 (2015) 1143–1169. https://doi.org/10.1002/adma.201403354.

[9] Y. Yang, Y. Cheng, S. Peng, L. Xu, C. He, F. Qi, M. Zhao, C. Shuai, Microstructure evolution and texture tailoring of reduced graphene oxide reinforced Zn scaffold,

Bioact. Mater. 6 (2021) 1230–1241. https://doi.org/10.1016/j.bioactmat.2020.10.017.

[10] C. Shuai, G. Liu, Y. Yang, F. Qi, S. Peng, W. Yang, C. He, G. Wang, G. Qian, A strawberry-like Ag-decorated barium titanate enhances piezoelectric and antibacterial activities of polymer scaffold, Nano Energy. 74 (2020) 104825. https://doi.org/10.1016/j.nanoen.2020.104825.

[11] Y. Deng, X. Gao, X.L. Shi, S. Lu, W. Yang, C. Duan, Z.G. Chen, Graphene Oxide and Adiponectin-Functionalized Sulfonated Poly(etheretherketone) with Effective Osteogenicity and Remotely Repeatable Photodisinfection, Chem. Mater. 32 (2020) 2180–2193. https://doi.org/10.1021/acs.chemmater.0c00290.

[12] S. Reed, B. Wu, Sustained growth factor delivery in tissue engineering applications, Ann. Biomed. Eng. 42 (2014) 1528–1536. https://doi.org/10.1007/s10439-013-0956-6.

[13] G.G. Walmsley, A. McArdle, R. Tevlin, A. Momeni, D. Atashroo, M.S. Hu, A.H. Feroze, V.W. Wong, P.H. Lorenz, M.T. Longaker, D.C. Wan, Nanotechnology in bone tissue engineering, Nanomedicine Nanotechnology, Biol. Med. 11 (2015) 1253–1263. https://doi.org/10.1016/j.nano.2015.02.013.

[14] H. Li, S. Pan, P. Xia, Y. Chang, C. Fu, W. Kong, Z. Yu, K. Wang, X. Yang, Advances in the application of gold nanoparticles in bone tissue engineering, (2020) 1–15.

[15] L. Dykman, N. Khlebtsov, Gold nanoparticles in biomedical applications: Recent advances and perspectives, Chem. Soc. Rev. (2012). https://doi.org/10.1039/c1cs15166e.

[16] D.N. Heo, N.J. Castro, S.J. Lee, H. Noh, W. Zhu, L.G. Zhang, Enhanced bone tissue regeneration using a 3D printed microstructure incorporated with a hybrid nano hydrogel, Nanoscale. 9 (2017) 5055–5062. https://doi.org/10.1039/c6nr09652b.

[17] H. Nekounam, Z. Allahyari, S. Gholizadeh, E. Mirzaei, M.A. Shokrgozar, R. Faridi-Majidi, Simple and robust fabrication and characterization of conductive carbonized

nanofibers loaded with gold nanoparticles for bone tissue engineering applications, Mater. Sci. Eng. C. 117 (2020) 111226. https://doi.org/10.1016/j.msec.2020.111226.

[18] K. Sehnal, M. Gargulak, A.E. Ofomaja, M. Stankova, B. Hosnedlova, C. Fernandez, M. Docekalova, J. Sochor, M. Kepinska, Z. Tothova, D.N. Bach, R. Kizek, D. Uhlirova, H.V. Nguyen, Biophysical analysis of silver nanoparticles prepared by green synthesis and their use for 3D printing of antibacterial material for health care, 2019 IEEE Int. Conf. Sensors Nanotechnology, SENSORS NANO 2019. (2019) 2019–2022. https://doi.org/10.1109/SENSORSNANO44414.2019.8940081.

[19] S. Radhakrishnan, S. Nagarajan, H. Belaid, C. Farha, I. Iatsunskyi, E. Coy, L. Soussan, V. Huon, J. Bares, K. Belkacemi, C. Teyssier, S. Balme, P. Miele, D. Cornu, N. Kalkura, V. Cavaillès, M. Bechelany, Fabrication of 3D printed antimicrobial polycaprolactone scaffolds for tissue engineering applications, Mater. Sci. Eng. C. 118 (2021) 111525. https://doi.org/10.1016/j.msec.2020.111525.

[20] J.H. Lee, J.M. Baik, Y.S. Yu, J.H. Kim, C.B. Ahn, K.H. Son, J.H. Kim, E.S. Choi, J.W. Lee, Development of a heat labile antibiotic eluting 3D printed scaffold for the treatment of osteomyelitis, Sci. Rep. 10 (2020). https://doi.org/10.1038/s41598-020-64573-5.

[21] N. Jiang, D.H. Dusane, J.R. Brooks, C.P. Delury, S.S. Aiken, P.A. Laycock, P. Stoodley, Antibiotic loaded β-tricalcium phosphate/calcium sulfate for antimicrobial potency, prevention and killing efficacy of Pseudomonas aeruginosa and Staphylococcus aureus biofilms, Sci. Rep. 11 (2021) 1–9. https://doi.org/10.1038/s41598-020-80764-6.

[22] R. Dorati, A. DeTrizio, T. Modena, B. Conti, F. Benazzo, G. Gastaldi, I. Genta, Biodegradable scaffolds for bone regeneration combined with drug-delivery systems in osteomyelitis therapy, Pharmaceuticals. 10 (2017) 96.

https://doi.org/10.3390/ph10040096.

[23] M. Sabitha, R. Sheeja, Preparation and characterization of ampicillin-incorporated electrospun polyurethane scaffolds for wound healing and infection control, Polym. Eng. Sci. 55 (2015) 541–548. https://doi.org/10.1002/pen.23917.

[24] B. Dorj, J.E. Won, O. Purevdorj, K.D. Patel, J.H. Kim, E.J. Lee, H.W. Kim, A novel therapeutic design of microporous-structured biopolymer scaffolds for drug loading and delivery, Acta Biomater. 10 (2014) 1238–1250. https://doi.org/10.1016/j.actbio.2013.11.002.

[25] V. Martin, I.A. Ribeiro, M.M. Alves, L. Gonçalves, R.A. Claudio, L. Grenho, M.H. Fernandes, P. Gomes, C.F. Santos, A.F. Bettencourt, Engineering a multifunctional 3D-printed PLA-collagen-minocycline-nanoHydroxyapatite scaffold with combined antimicrobial and osteogenic effects for bone regeneration, Mater. Sci. Eng. C. 101 (2019) 15–26. https://doi.org/10.1016/j.msec.2019.03.056.

[26] A.O. Basar, V. Sadhu, H. Turkoglu Sasmazel, Preparation of electrospun PCL-based scaffolds by mono/multi-functionalized GO, Biomed. Mater. 14 (2019) 045012. https://doi.org/10.1088/1748-605X/ab2035.

[27] M. Gozutok, V. Sadhu, H.T. Sasmazel, Development of Poly(vinyl alcohol) (PVA)/Reduced Graphene Oxide (rGO) Electrospun Mats, J. Nanosci. Nanotechnol. 19 (2019) 4292–4298. https://doi.org/10.1166/jnn.2019.16290.

[28] M.A. Teixeira, M.T.P. Amorim, H.P. Felgueiras, Poly (Vinyl Alcohol) -Based Nanofibrous Electrospun Sca ff olds for Tissue Engineering Applications, Polymers (Basel). 12 (2020) 7. https://doi.org/10.3390/polym12010007.

[29] E. Dattola, E.I. Parrotta, S. Scalise, G. Perozziello, T. Limongi, P. Candeloro, M.L. Coluccio, C. Maletta, L. Bruno, M.T. De Angelis, G. Santamaria, V. Mollace, E. Lamanna, E. Di Fabrizio, G. Cuda, Development of 3D PVA scaffolds for cardiac

tissue engineering and cell screening applications, RSC Adv. 9 (2019) 4246–4257. https://doi.org/10.1039/C8RA08187E.

[30] N.S.N.H. Nizan, F.H. Zulkifli, Reinforcement of hydroxyethyl cellulose / poly (vinyl alcohol) with cellulose nanocrystal as a bone tissue engineering scaffold, J. Polym. Res. 27 (2020) 169. https://doi.org/10.1007/s10965-020-02112-6.

[31] A. Goyanes, M. Kobayashi, R. Martínez-Pacheco, S. Gaisford, A.W. Basit, Fused-filament 3D printing of drug products: Microstructure analysis and drug release characteristics of PVA-based caplets, Int. J. Pharm. 514 (2016) 290–295. https://doi.org/10.1016/j.ijpharm.2016.06.021.

[32] T. Tagami, N. Nagata, N. Hayashi, E. Ogawa, K. Fukushige, N. Sakai, T. Ozeki, Defined drug release from 3D-printed composite tablets consisting of drug-loaded polyvinylalcohol and a water-soluble or water-insoluble polymer filler, Int. J. Pharm. 543 (2018) 361–367. https://doi.org/10.1016/j.ijpharm.2018.03.057.

[33] M. Merchan, J. Sedlarikova, M. Friedrich, V. Sedlarik, P. Saha, Thermoplastic modification of medical grade polyvinyl chloride with various antibiotics: Effect of antibiotic chemical structure on mechanical, antibacterial properties, and release activity, Polym. Bull. 67 (2011) 997–1016. https://doi.org/10.1007/s00289-011-0474-3.

[34] G. Turnbull, J. Clarke, F. Picard, P. Riches, L. Jia, F. Han, B. Li, W. Shu, 3D bioactive composite scaffolds for bone tissue engineering, Bioact. Mater. 3 (2018) 278–314. https://doi.org/10.1016/j.bioactmat.2017.10.001.

[35] S.J. Lee, H.J. Lee, S.Y. Kim, J.M. Seok, J.H. Lee, W.D. Kim, I.K. Kwon, S.Y. Park, S.A. Park, In situ gold nanoparticle growth on polydopamine-coated 3D-printed scaffolds improves osteogenic differentiation for bone tissue engineering applications: In vitro and in vivo studies, Nanoscale. 10 (2018) 15447–15453. https://doi.org/10.1039/c8nr04037k.

[36] G. Li, L. Wang, W. Pan, F. Yang, W. Jiang, X. Wu, X. Kong, K. Dai, Y. Hao, In vitro and in vivo study of additive manufactured porous Ti6Al4V scaffolds for repairing bone defects, Sci. Rep. 6 (2016) 34072. https://doi.org/10.1038/srep34072.

[37] H. Awada, C. Daneault, Chemical Modification of Poly(Vinyl Alcohol) in Water, Appl. Sci. 5 (2015) 840–85. https://doi.org/10.3390/app5040840.

[38] H.S. Mansur, C.M. Sadahira, A.N. Souza, A.A.P. Mansur, FTIR spectroscopy characterization of poly (vinyl alcohol) hydrogel with different hydrolysis degree and chemically crosslinked with glutaraldehyde, Mater. Sci. Eng. C. 28 (2008) 539–548. https://doi.org/10.1016/j.msec.2007.10.088.

[39] A. Bernal-Ballen, J. Lopez-Garcia, M.A. Merchan-Merchan, M. Lehocky, Synthesis and characterization of a bioartificial polymeric system with potential antibacterial activity: Chitosan-polyvinyl alcohol-ampicillin, Molecules. 23 (2018) 3109. https://doi.org/10.3390/molecules23123109.

[40] W.N.W. Shukri, N. Bidin, S. Islam, G. Krishnan, M.A.A. Bakar, M.S. Affandi, Synthesis and characterization of uncoated and cysteamine-coated gold nanoparticles by pulsed laser ablation, J. Nanophotonics. 10 (2016) 046007. https://doi.org/10.1117/1.jnp.10.046007.

[41] V. Nairi, L. Medda, M. Monduzzi, A. Salis, Adsorption and release of ampicillin antibiotic from ordered mesoporous silica, J. Colloid Interface Sci. 497 (2017) 217–225. https://doi.org/10.1016/j.jcis.2017.03.021.

[42] S. Krishnamurthy, A. Esterle, N.C. Sharma, S. V. Sahi, Yucca-derived synthesis of gold nanomaterial and their catalytic potential, Nanoscale Res. Lett. 9 (2014) 627. https://doi.org/10.1186/1556-276X-9-627.

[43] C. Li, Z. Li, Y. Wang, H. Liu, Gold Nanoparticles Promote Proliferation of Human Periodontal Ligament Stem Cells and Have Limited Effects on Cells Differentiation, J.

Nanomater. 2016 (2016) 1–10. https://doi.org/10.1155/2016/1431836.

[44] S. Singh, A. Gupta, I. Qayoom, A.K. Teotia, S. Gupta, P. Padmanabhan, A. Dev, A. Kumar, Biofabrication of gold nanoparticles with bone remodeling potential: an in vitro and in vivo assessment, J. Nanoparticle Res. 22 (2020) 152. https://doi.org/10.1007/s11051-020-04883-x.

[45] Y. Zhang, P. Wang, H. Mao, Y. Zhang, L. Zheng, P. Yu, Z. Guo, L. Li, Q. Jiang, PEGylated gold nanoparticles promote osteogenic differentiation in in vitro and in vivo systems, Mater. Des. 197 (2021) 109231. https://doi.org/10.1016/j.matdes.2020.109231.

[46] Bernal-ballen, J.-A. Lopez-Garcia, K. Ozaltin, polymers Polymeric Material with Combined Properties in Cell Regeneration and Potential Antibacterial Features, Polymers (Basel). 1325 (2019) 1–14.

[47] J. Shao, J. Ma, L. Lin, B. Wang, J.A. Jansen, X.F. Walboomers, Y. Zuo, F. Yang, Three-Dimensional Printing of Drug-Loaded Scaffolds for Antibacterial and Analgesic Applications, Tissue Eng. - Part C Methods. 25 (2019) 222–231. https://doi.org/10.1089/ten.tec.2018.0293.

[48] D. Zhang, D. Liu, J. Zhang, C. Fong, M. Yang, Gold nanoparticles stimulate differentiation and mineralization of primary osteoblasts through the ERK/MAPK signaling pathway, Mater. Sci. Eng. C. 42 (2014) 70–77. https://doi.org/10.1016/j.msec.2014.04.042.

[49] H. Nah, D. Lee, M. Heo, J.S. Lee, S.J. Lee, D.N. Heo, J. Seong, H.N. Lim, Y.H. Lee, H.J. Moon, Y.S. Hwang, I.K. Kwon, Vitamin D-conjugated gold nanoparticles as functional carriers to enhancing osteogenic differentiation, Sci. Technol. Adv. Mater. 20 (2019) 826–836. https://doi.org/10.1080/14686996.2019.1644193.

[50] Y. Fan, A.C. Pauer, A.A. Gonzales, H. Fenniri, Enhanced antibiotic activity of

ampicillin conjugated to gold nanoparticles on PEGylated rosette nanotubes, Int. J. Nanomedicine. 14 (2019) 7281–7289. https://doi.org/10.2147/IJN.S209756.

[51] N. Tarrat, M. Benoit, M. Giraud, A. Ponchet, M.J. Casanove, The gold/ampicillin interface at the atomic scale, Nanoscale. 7 (2015) 14515–14524. https://doi.org/10.1039/c5nr03318g.

[52] E.S. Elmolla, M. Chaudhuri, Degradation of amoxicillin, ampicillin and cloxacillin antibiotics in aqueous solution by the UV/ZnO photocatalytic process, J. Hazard. Mater. 173 (2010) 445–449. https://doi.org/10.1016/j.jhazmat.2009.08.104.

[53] S. Naveed, S. Uroog, N. Waheed, Degradation studies of different brands of moxifloxac in available in the market, Int. J. Curr. Pharm. Rev. Res. 5 (2015) 110–116.

Declaration of interests

☒ The authors declare that they have no known competing financial interests or personal relationships that could have appeared to influence the work reported in this paper.

☐The authors declare the following financial interests/personal relationships which may be considered as potential competing interests:

CRediT author statement

Aysenur Topsakal: Conceptualization, Methodology, Data curation, Visualization, Investigation, Writing- Original draft preparation. **Swati Midha:** Data curation, Visualization, Writing- Original draft preparation and Editing **Esra Yuca:** Supervision, Resources, Writing- Reviewing and Editing **Hilal Turkoğlu Sasmazel:** Supervision, Resources, Conceptualization. **Arı Tukay:** Data curation, Visualization, Investigation, Conceptualization, Writing. **Deepak Kalaskar:** Supervision, Data Curation, Conceptualization, Project administration, Writing- Reviewing and Editing **Oguzhan Gunduz:** Supervision, Resources, Data Curation, Conceptualization, Project administration, Writing- Reviewing and Editing, Funding acquisition.